JOURNAL OF EXPERIMENTAL AND THEORETICAL PHYSICS, 2024, Vol. 166, No. 6 (12), pp. 753–762

ATOMS, MOLECULES, OPTICS

OPTICAL CONTROL OF NANOPARTICLE DISTRIBUTION IN COLLOIDS WITH GAIN AND ABSORPTION

© 2024 A. A. Zharov[a], N. A. Zharova[b]*

[a] Institute for Physics of Microstructures of the Russian Academy of Sciences, Nizhny Novgorod, 603950 Russia
[b] Institute of Applied Physics of the Russian Academy of Sciences, Nizhny Novgorod, 603950 Russia
*e-mail: zhani@appl.sci-nnov.ru

Received June 05, 2024
Revised August 04, 2024
Accepted August 14, 2024

Abstract. The effect of light on a composite system, which is an absorption/gain-balanced colloidal solution of absorbing nanoparticles in a gain medium, is studied. A model of a flat colloidal layer with normally incident plane (TEM) electromagnetic wave is considered. The combined action of striction and drag force (force arising from the transfer of photon momentum to absorbing particles) causes spatial redistribution of particle concentration, resulting in local disruption of absorption and gain balance in the layer, and spatial regions where light amplification and absorption occur are distinguished. It is shown that depending on the incident radiation intensity, both smooth and almost step-like nanoparticle concentration profiles can be realized. The corresponding distributions of the effective dielectric permittivity of the colloid possess PT (Parity-Time)-symmetry (satisfying condition $\varepsilon(z) = \varepsilon^*(-z)$) at low pump field intensity, but differ from PT-symmetric distributions at moderate and high intensities. Creating a controlled profile of local light gain and absorption can serve as a platform for studying specific non-Hermitian optical effects, and also expands the possibilities of optical diagnostics of nanoparticle distribution in colloidal solutions with compensated absorption.

DOI: 10.31857/S004445102412e022

1. INTRODUCTION

Managing losses and especially creating conditions for the propagation of undamped optical modes is a long-standing but still relevant problem in optics. Full compensation of spatially inhomogeneous losses through the inclusion of active optical elements (pumping) in the system is individual in nature: in principle, each mode requires its own pumping profile. However, there exists an entire class of PT (Parity-Time)-symmetric systems (invariant with respect to spatial coordinate inversion and time reversal [1]), in which such compensation (for PT-symmetric modes) is achieved automatically.

The concept of PT-symmetry originates from quantum mechanics [2], where it was shown that a hypothetical complex PT-symmetric potential can have states (also PT-symmetric eigenfunctions) with real eigenvalues. In optics, for quasi-monochromatic ($\propto \exp(i\omega t)$) processes, time reversal corresponds to sign reversal of the imaginary unit, and PT-symmetry satisfies the condition determining a specific spatial distribution of real and imaginary parts of the dielectric permittivity, $\varepsilon(\mathbf{r}) = \varepsilon^*(-\mathbf{r})$ [3].

Theoretical and experimental studies have shown that changing parameters in a PT-symmetric system (usually the growth of the imaginary part of permittivity, both positive and negative) can lead to breaking of the PT-symmetry of the mode and transformation of its spectrum from purely real to complex. The corresponding transition point, where eigenvalue degeneracy occurs, is commonly called an "exceptional point," and the transition itself from real to complex eigenvalues can be interpreted as a second-order phase transition [4].

The experimental accessibility of optical PT-symmetric systems and, in particular, the effect of exceptional points has given rise to several new applications, such as devices for induced absorption and amplification [1,5,6], non-reciprocal photon transport [7], sensing [8], etc. Currently, optical PT-symmetric structures are produced based on III-V group semiconductor materials [6] or doped silicon crystal [9].

In this work, we propose a model of a non-Hermitian optical system based on a tunable and configurable liquid metamaterial (a colloidal solution of absorbing particles in an amplifying fluid [10]), which under the influence of light can exhibit both PT-symmetric and non-PT-symmetric distributions of dielectric permittivity.

A similar problem formulation was used in the authors' recent work [11], where a colloid with suspended particles of two types (amplifying and absorbing) was considered as a metamaterial medium, which provided zero balance of gain-absorption. Under the influence of light in such a system, absorbing particles experience a drag force directed along the wave vector and associated with photon momentum transfer, while the force acting on active particles is directed in the opposite direction and appears as a result of stimulated emission [12-14]. In [11], it was shown that the redistribution of the spatial density of amplifying and absorbing particles under the action of these forces always leads to the formation of a PT-symmetric profile of effective dielectric permittivity.

A more realistic model of the medium used in the present work assumes that light amplification is achieved through a photoactive gel [15] and remains spatially uniform, while the structural inhomogeneity of the medium appears due to drag and striction forces acting on absorbing particles. Unlike [11], here we do not limit ourselves to linear approximation when calculating particle dynamics.

As will be shown below, at high radiation intensity, a strongly nonlinear regime is established, in which the perturbation of particle concentration can become comparable to and greater than the unperturbed density. This leads to the possibility of forming both smooth and quasistep-like particle concentration profiles, which may possess PT-symmetry or differ from it. This gives grounds to consider such a tunable system as a platform for studying specific non-Hermitian optical effects, as well as for diagnosing spatial distributions of nanoparticles using probe waves.

2. PROBLEM STATEMENT

We consider the scattering of electromagnetic radiation by a flat layer of composite medium, which represents a colloidal solution of absorbing nanoparticles in an active fluid (gel). The fluid provides amplification of electromagnetic waves such that in equilibrium state, when particles are uniformly distributed throughout the volume, losses and amplification are compensated, and on average, the medium neither amplifies nor weakens the radiation passing through it.

The effective dielectric permittivity of the medium in dipole approximation at sufficiently low concentration of nanoparticles can be written as

$$\varepsilon \cong \varepsilon_0 + V[\alpha(1+n) + i\tilde{\alpha}n], \tag{1}$$

where ε_0 — is the real part of fluid permittivity without particles, $V = 4\pi b^3 N_0/3$ is the volume fraction of particles in the fluid, N_0 is the average volumetric concentration of nanoparticles, b is the particle radius (for simplicity, we assume that particles have spherical shape), α and $\tilde{\alpha}$ are the real and imaginary parts of particle polarizability, and we introduced dimensionless variable $n = N/N_0 - 1$, characterizing deviation of local particle density N from equilibrium value N_0. Here it is also taken into account that in a homogeneous medium ($n = 0$) absorption and amplification are compensated, $\mathrm{Im}\,\varepsilon = 0$.

The fluid component of the medium provides amplification, while nanoparticles are responsible for absorption. However, each individual particle in the process of electromagnetic wave absorption receives not only its energy but also momentum. As a result, an effective drag, or scattering force acts on the particle. This force and associated radiation pressure effect are manifested in experiments on laser cooling and trapping of neutral particles [16], separation, detection, and sorting of nanoparticles [17, 18]. Obviously, the drag force is proportional to the product of electromagnetic field energy flux density and absorption coefficient (imaginary part of particle dipole moment).

In quasi-static approximation, the expression for drag force has the form

$$F^{sc} = -i\tilde{\alpha}\frac{b^3}{6}\left(E\frac{\partial E^*}{\partial z} - E^*\frac{\partial E}{\partial z}\right) = \tilde{\alpha}\frac{b^3}{3}\mathrm{Im}\left(E^*\frac{\partial E}{\partial z}\right). \tag{2}$$

Additionally, particles are also affected by ponderomotive gradient (striction) force

$$F^{grad} = \alpha \frac{b^3}{3} \mathrm{Re}\left(E^* \frac{\partial E}{\partial z}\right) = \alpha \frac{b^3}{6} \nabla |E|^2. \quad (3)$$

The gradient force is not related to absorption but leads, depending on the sign of α either to particles being drawn into the strong field region or being pushed out of this region[1].

Under the influence of these forces and the thermal pressure gradient, particles begin to move, and in a viscous medium, their velocity u is determined from the equation of motion

$$\frac{\partial u}{\partial t} + \frac{u}{\tau} = \frac{F^{grad} + F^{sc}}{m} - V_T^2 \frac{\partial n / \partial z}{1+n}, \quad (4)$$

where τ is the characteristic velocity relaxation time of particles in a viscous fluid, m is the particle mass, $V_T = \sqrt{k_B T/m}$ is the thermal velocity, k_B is the Boltzmann constant, T — temperature.

During electromagnetic radiation propagation in the medium, there will be a redistribution of nanoparticle concentration, which, in turn, will lead to the appearance of local areas with amplification and absorption within the layer. In the steady state, the particle concentration distribution will satisfy the equation

$$\frac{F^{grad} + F^{sc}}{m} = V_T^2 \frac{n'}{1+n}, \quad (5)$$

where the prime denotes spatial derivative $\partial/\partial z$.

3. BOUNDARY VALUE PROBLEM: FINITE THICKNESS LAYER

Let's consider normal incidence of a plane (TEM) electromagnetic wave on a layer of thickness L ($-L/2 \le z \le L/2$). We assume that outside the layer, the dielectric permittivity is $\varepsilon = 1$. Under the influence of electromagnetic radiation (striction and drag force), a steady state with inhomogeneous particle concentration is established, $n \neq 0$. It is important to note that the redistribution of particles in the layer does not change their total number, so the concentration perturbation averaged over the layer thickness equals zero,

$$\int_{-L/2}^{L/2} n dz = 0.$$

In the slowly varying amplitude approximation, the field inside the layer is a superposition of plane waves propagating in forward and backward directions along z,

$$E = A_+(z)\exp(ikz) + A_-(z)\exp(-ikz),$$

where complex amplitudes

$$A_\pm \equiv a_\pm \exp(i\phi_\pm)$$

vary weakly over the wavelength,

$$|A_\pm'| \ll k|A_\pm|, \quad k = k_0\sqrt{\varepsilon_0 + V\alpha},$$

$k_0 = \omega/c$, c is the speed of light. In this case, we can approximately write [2]

$$E^* E' \approx ika_+^2 + a_+ a_+' + i\phi_+' a_+^2 - ika_-^2 + a_- a_-' + i\phi_-' a_-^2$$

and, substituting this expression into (5), obtain the relation [3]

$$\frac{n'}{1+n} = \alpha(a_+^2 + a_-^2)' + \tilde{\alpha}[k(a_+^2 - a_-^2) + \phi_+' a_+^2 + \phi_-' a_-^2], \quad (6)$$

where the contribution from terms $\phi_\pm' a_\pm^2$ to concentration change can be neglected since $\phi_\pm' \ll k$.

Light propagation in the layer is described by the wave equation,

$$d^2E/dz^2 + k_0^2 \varepsilon E = 0,$$

which in the first order of smallness in perturbation amplitude takes the form

$$\pm 2ik(a_\pm' + i\phi_\pm' a_\pm) + k_0^2 V(\alpha(1+n) + i\tilde{\alpha}n)a_\pm = 0. \quad (7)$$

[1] Nanoparticles absorb light radiation, therefore the coefficient $\tilde{\alpha}$ must be positive, $\tilde{\alpha} > 0$. The positive sign of the striction parameter α indicates that particles should be drawn into the region of strong field. This is true for dielectric particles, however the sign of α may change in case of metallic nanoparticles.

[2] Further, we consider the electric field normalized to the value $E_c = \sqrt{6k_B T/b^3}$.

[3] Although, as noted above, the concentration of nanoparticles is assumed to be small, the relative perturbation of concentration can be significant, up to complete expulsion of particles from some local area. Therefore, we take into account the term n in the denominator of expression (6).

Separating real and imaginary parts in equation (7), we obtain

$$\frac{(a_+^2)'}{a_+^2} = -\Gamma n, \ \frac{(a_-^2)'}{a_-^2} = \Gamma n, \qquad (8)$$
$$\phi_\pm' = \pm\,\Gamma(\alpha/2\tilde{\alpha})(1+n),$$

where

$$\Gamma = k_0^2\tilde{\alpha}V/k.$$

Adding the first two equations of (8), we find that within the used approximations, the product of wave amplitudes propagating along z and in the opposite direction does not depend on z:

$$a_+^2 a_-^2 = C. \qquad (9)$$

Here C is a constant which, as will be shown below, is determined by the continuity conditions of electric and magnetic fields at the layer boundaries.

It is convenient to present the main system of equations in dimensionless form with a minimum number of coefficients. The corresponding normalization of the spatial variable, $\tilde{z} = \Gamma z$ (henceforth we omit the sign $\tilde{}$), allows us to write the first equation of system (7) in the form

$$\frac{s'}{s} = -n, \qquad (10)$$

where we introduced the quantity $s \equiv a_+^2$. The equation for concentration (6) can be rewritten taking into account the local relation of amplitudes (9), $a_-^2 = C/s$, as

$$\frac{n'}{1+n} = \gamma\left[(s - C/s) + \frac{\alpha}{k\tilde{\alpha}}(s + C/s)'\right] = \gamma\,(s - C/s)(1 - \beta n) \qquad (11)$$

with coefficients

$$\gamma = k\tilde{\alpha}/\Gamma, \quad \beta = \alpha\Gamma/(k\tilde{\alpha}).$$

Division of expression (10) by (11) gives the differential relation between s and n:

$$\gamma\frac{(s - C/s)ds}{s} = -\frac{ndn}{(1+n)(1-\beta n)}. \qquad (12)$$

This relation can be integrated resulting in

$$\frac{\log|1+n| + (1/\beta)\log|1-\beta n|}{\gamma(1+\beta)} - \left(s + \frac{C}{s}\right) = \text{const}. \qquad (13)$$

Replacing n with $-s'/s$, in the last formula, we find the dependence $s'(s)$:

$$\frac{\log|1 - s'/s| + (1/\beta)\log|1 + \beta s'/s|}{\gamma(1+\beta)} - \left(s + \frac{C}{s}\right) = \text{const}, \qquad (14)$$

and thus obtain the phase plane of the initial system.

For the analysis of the solution on the phase plane, first note that for values $n = -1$ and $n = 1/\beta$ the expression in the left part of equation (13) becomes infinite in absolute value. Accordingly, on the plane (s', s) the straight lines defined by equations $s' = s$ and $s' = -s/\beta$, divide the phase plane into three sectors: $s' < -s/\beta$, $-s/\beta < s' < s$ and $s < s'$. Phase trajectories cannot cross the boundaries between sectors, therefore only solutions related to the central sector have physical meaning, where phase trajectories pass through regions with both positive and negative values of s'. In the other two sectors s' (and correspondingly $n = -s'/s$) does not change sign, making it impossible to satisfy the condition of zero concentration averaged over any segment of the phase trajectory.

Fig. 1 shows an example of the phase plane of the system of equations for parameters $C = 2$, $\beta = 2$, $\gamma = 0.0125$. The corresponding values of the constant in (14) are -10 (curve 1), -20 (curve 2) and -30 (curve 3).

The slow amplitude approximation assumes that waves propagating in the positive and negative directions along the z, axis do not interact within the layer; they can only exchange energy at the boundaries. In the problem of incident radiation scattering on a layer, the boundary conditions at $z = L/2$ are written as

$$a_-/a_+(z = L/2) = \mu,$$

where $\mu = (k-1)/(k+1)$ and $k = \sqrt{\varepsilon}$. Thus, at the layer boundary, the ratio of harmonics amplitudes propagating in positive and negative directions is determined by the material parameters of the layer and surrounding medium (recall that the dielectric permittivity of the surrounding medium equals 1). On the other hand, for any point inside the layer, including the boundary, we have from relation (9)

$$a_+^2 a_-^2 = C.$$

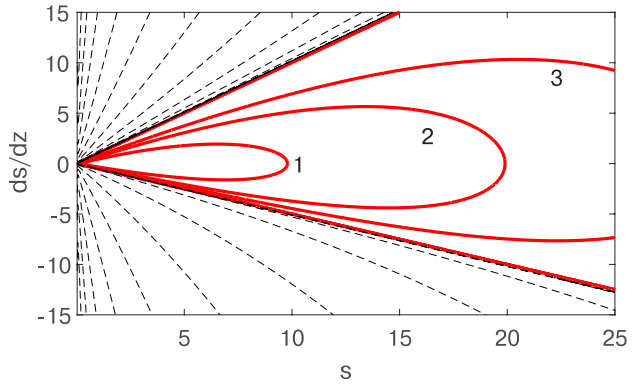

Fig. 1. Phase plane of the system of equations (10), (11) for parameters $C = 2$, $\beta = 2$, $\gamma = 0.0125$. The corresponding values of the constant in (14) are -10 (curve 1), -20 (curve 2), 30 (curve 3). Phase trajectories relating to the upper and lower sectors of the phase plane have no physical meaning, since on any segment of such trajectories, the integral of s'/s (of particle concentration) is not equal to zero

From relations (8), we can find the dependence of amplitudes on z,

$$a_{\pm}^2(z) = a_{\pm}^2(-L/2)\exp\left(\mp\Gamma\int\limits_{-L/2}^{z} n dz\right),$$

and note that the amplitudes at the boundaries are equal

$$a_+(z = L/2) = a_+(z = -L/2),$$
$$a_-(z = L/2) = a_-(z = -L/2),$$

since

$$\int\limits_{-L/2}^{L/2} n dz = 0$$

(the number of particles in the layer is conserved). Thus, the layer neither amplifies nor attenuates radiation.

Solving the linear problem of incident wave scattering with amplitude A_{inc} on the layer, we obtain the relationship between $a_{\pm}$ and A_{inc}:

$$2A_{inc} = \sqrt{s_0}(1+k)\left|1 - \mu^2\exp(2ikL)\right|, \quad (15)$$
$$a_-(z = \pm L) = \mu a_+(z = \pm L), \quad C = \mu^2 s_0^2,$$

where

$$s_0 = a_+^2(z = -L/2).$$

These relations completely determine the connection between the problem constants and physical parameters. We should note once again that the reflection and transmission coefficients, even in a strongly nonlinear case, turn out to be the same as in radiation scattering on a layer with undisturbed dielectric permittivity, and for an external observer, nonlinear effects inside the layer are not manifested in any way.

4. APPROXIMATE SOLUTION

In the case of $\beta = 1$, when the problem is PT-symmetric, it is not difficult to find a complete solution in linear approximation with respect to parameters $s - s_0$, n. The simplified system of equations

$$s' = -ns_0, n' = \gamma(s - C/s)$$

reduces to a harmonic equation for the quantity ν [4],

$$\nu = \int\limits_{-L/2}^{z} n dz,$$

$$\nu'' = \gamma s_0(1 - \nu - (1+\nu)\mu^2) \quad (16)$$

and has a solution in the form of

$$\nu = A + B\cos(\kappa z)$$

with the parameters

$$\kappa = \sqrt{\gamma s_0(1+\mu^2)},$$
$$A = (1-\mu^2)/(1+\mu^2),$$
$$B = -A/\cos(\kappa L/2).$$

As a result, for $n = \nu'$ we obtain

$$n = \frac{1-\mu^2}{1+\mu^2}\kappa\frac{\sin(\kappa z)}{\cos(\kappa L/2)}.$$

Obviously, if $\kappa L = m\pi$ $(m = 1,2,3,\ldots)$, then this solution is not applicable. At first glance, for small $\kappa \ll 1$, excluding resonance points, $\kappa L \neq m\pi$, this formula can be used since all applicability conditions are met, but this is not the case. When obtaining the simplified equation (16), we used the condition $\nu \ll 1$, and in this case, the right-hand side of the formula will be almost constant and does

[4] If $\beta \neq 1$, then under the same approximations, the main equation is replaced by the equation of a harmonic oscillator with damping ($\beta > 1$) or with pumping ($\beta < 1$), and the analytical solution appears rather cumbersome.

not change sign, while the left-hand side contains the derivative of concentration with respect to coordinate. Thus, we effectively assumed that $n'(z)$ is a sign-constant function, and accordingly $n(z)$ is a monotonic function. On the other hand, formal use of the obtained analytical solution indicates that as parameter $\kappa L > \pi$ increases, the profile $n(z)$ becomes non-monotonic (at large L may include even several periods of sine). Numerical investigation confirms that such non-monotonic concentration distributions are not realized, so a rough estimate of the applicability of the found solution reduces to the inequality $\kappa L/\pi < 1$.

An approximate solution can also be found in another limiting case of strong concentration perturbations and strong fields. The resulting structure can significantly differ from the PT-symmetric one. Numerical investigation (see below) shows that at large L and s_0 the particle density N has a step-like form with almost zero concentration in the layer region $-L/2 < z < z_{st}$ (near the radiation entry point) and constant density in the remaining part of the layer. Assuming that the concentration profile has a step structure

$$N \approx \begin{cases} 0, & -L/2 < z < z_{st}, \\ N_{max}, & z_{st} < z < L/2, \end{cases}$$

where z_{st} is the density jump coordinate, and N_{max} is the maximum density in the layer, both of these parameters can be found. The step position

$$z_{st}/L = 0.5(1-\beta)/(1+\beta)$$

is determined from the particle number conservation condition, and the value

$$N_{max} = 1 + 1/\beta$$

is found from formula (11), if we set $n' = 0$ in it. Note that at small β the particle localization region compresses, approaching the layer's output boundary. The exponential growth of the field in the region $z < z_{st}$,

$$s = s_0 \exp(z + L/2),$$

at $z > z_{st}$ is replaced by its exponential decay,

$$s = s_0 \exp\,[z_{st} - (N_{max}/N_0 - 1)z].$$

5. NUMERICAL SOLUTION

To find the stationary distribution of field intensity and concentration, the system of firstorder differential equations (10), (11) was solved numerically. At the input boundary of the layer $z = -L/2$ the values

$$a_+^2(-L/2) = s_0, \quad a_-^2(-L/2) = C/s_0$$

(see (15)) were set, found from solving the scattering problem of the incident wave on the unperturbed layer, as well as the perturbation of particle concentration $n_0 = n(-L/2)$. Unlike parameters s_0 and C, the value n_0 cannot be directly determined through physical (external) parameters of the problem, but it is also obvious that it cannot be arbitrary. An additional condition determining n_0, is the conservation of the number of particles in the layer, $\langle n \rangle = 0$. However, to verify this condition, one first needs to solve the problem and find the dependence $n(z)$ over the entire interval from $-L/2$ to $L/2$. Therefore, the numerical solution has to be found for an array of values n_0 (from -1 to 0) and then select from this set of solutions those that satisfy the condition $\langle n \rangle = 0$.

At fixed layer thickness and (normalized) material parameters γ, β (see system of equations (10), (11)), which characterize amplification in the active medium and the role of striction relative to the drag force, it is interesting to find the dependence of the stationary solution on the incident wave intensity. To obtain an answer to this question, one should repeatedly perform the procedure described above for a two-dimensional array of parameters (n_0, s_0) and obtain the resulting curve $n^*(s_0)$ on the plane (n_0, s_0).

This procedure was performed for a set of parameters $L = 9$, $\gamma_0 = 1.25 \cdot 10^{-2}$, $k = 2$, $\beta = 0.6$, and the calculation results are shown in Fig. 2. It turns out that the stationary solution is not always unique. There exists a range of incident wave intensities (in the figure, this approximately corresponds to the interval s_0 from 1.5 to 3.5), where there are three such stationary solutions, and the dependence $n^*(s_0)$ has a characteristic hysteresis curve shape (see Fig. 2*a*). The hysteresis effect is also manifested in the dependence of the maximum field intensity value inside the layer on the input intensity, which is shown as an example in Fig. 2*b*. The corresponding structure of the

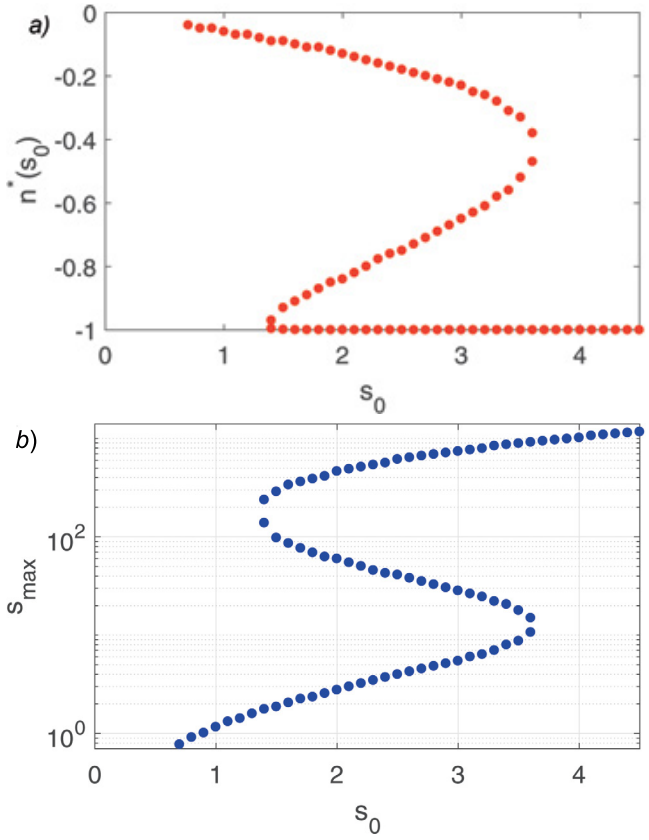

Fig. 2. *a* – Numerically found dependence $n^*(s_0)$: for each value of input power (and according to (15) for each s_0) the stationary distribution of field and particles is established if the particle density perturbation at $z = -L/2$ equals $n^*(s_0)$. *b* – Maximum value of radiation intensity inside the layer depending on s_0. The ambiguous nature of the dependence indicates the hysteresis effect. The following parameters were used for numerical simulation: $L = 9, \gamma_0 = 1.25 \cdot 10^{-2}, k = 2, \beta = 0.6$

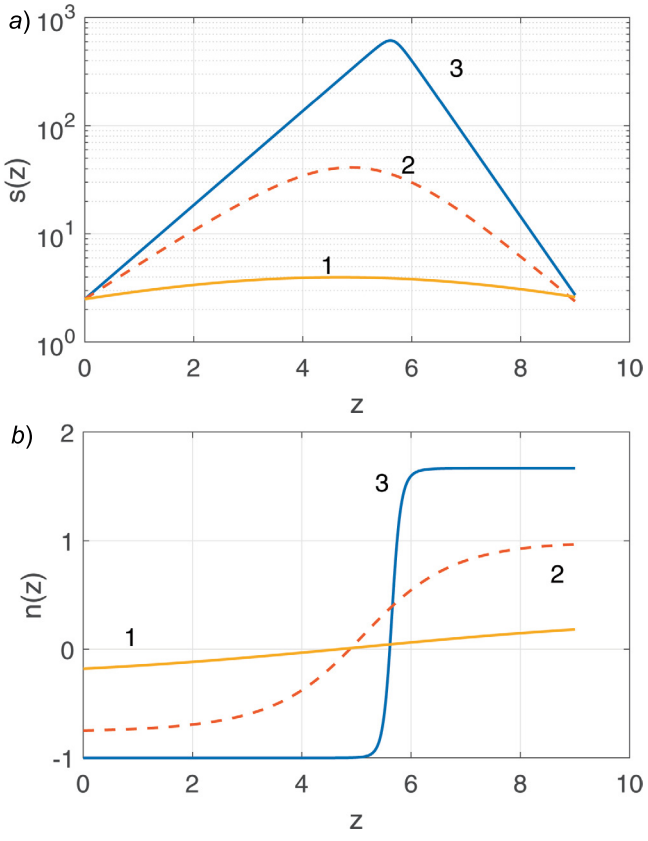

Fig. 3. Structure of multistable solution with parameter $s_0 = 2.5$. At the corresponding intensity (see (15)), there exists not one but three stationary solutions that differ significantly in maximum field amplitude and particle concentration profile. *a* – Dependence $s(z)$ (logarithmic scale): while curves 1 and 2 show relatively small field amplification, curve 3 demonstrates local intensity amplification at maximum $s_{max}/s_0 \approx 200$. It should also be noted for this case a noticeable violation of PT-symmetry, which, however, does not lead to any field amplification over the full layer length. *b* – Dependence $n(z)$ for three stationary solutions: almost linearly growing with increasing coordinate z weak concentration perturbation corresponds to the solution with minimal field amplification, while maximum amplification is achieved when practically all absorbing particles are displaced to the region $z > L/(1+\beta)$, and a step-like concentration profile is formed. The following parameters were used for numerical modeling: $L = 9, \gamma_0 = 1.25 \cdot 10^{-2}, k = 2, \beta = 0.6$

three potentially possible stationary solutions is shown in Fig. 3: for one input power of the incident radiation P_{in} (P_{in} is proportional to s_0, see (15)) the stationary distributions of particle density and field intensity inside the layer differ significantly, with the maximum field intensity amplification in these solutions differing by orders of magnitude (here approximately by a factor of 100). Additionally, in different stationary states, the concentration profile $N(z)$ changes significantly and the PT-symmetry violation becomes noticeable.

To determine which of these stationary states is realized, it is necessary to solve a dynamic problem where external radiation falls on an unperturbed initial profile $N(z) = N_0$. The evolution of particle density is described by a nonlinear diffusion equation derived from the particle motion equation and continuity equation

$$\frac{1}{\tau}\frac{\partial n}{\partial t} = \frac{\partial}{\partial z}\left[\frac{\partial n}{\partial z} - \gamma(s - C/s)(1+n)(1-\beta n)\right], \quad (17)$$

which is the (normalized) continuity equation

$$\partial N/\partial t + \partial/\partial z(Nu) = 0,$$

where particle velocity is given by expression (4).

In calculations, we assume that the value s_0 remains constant in time (incident radiation is abruptly "switched on" at time moment $t = 0$ and its power does not change thereafter), while radiation

intensity inside the layer, as before, is determined by expression (10), i.e., depends on the concentration profile of absorbing particles at each given moment of time.

Bistability is a fairly common phenomenon in nonlinear systems [19]. In the standard problem formulation, a slow change (increase or decrease) in input power is assumed. The study of the system's temporal dynamics shows that with increasing input power, a stationary solution is realized with the smallest possible perturbation of concentration and corresponding (smallest possible) field intensity amplification inside the layer. Similarly, if slowly decreasing the intensity of incident radiation (value s_0), the maximally perturbed distribution of particles and field will be established. The intermediate branch of solutions is unstable, so in the parameter region where the solution is not unique, the system is bistable. Obviously, in this case, going beyond the bistability boundary (in Fig. 2 at $s_0 \approx 1.5$ and $s_0 \approx 3.5$) is accompanied by a sharp restructuring of the stationary solution.

It should be noted that the results can be significantly influenced by the gain saturation effect if large fields are achieved inside the layer. To account for this effect, the following approximate formula for the local gain coefficient can be used:

$$\gamma = \frac{\gamma_0}{1 + P/P_{satur}},$$

where γ_0 is the gain of weak signals (increment without considering saturation), P is the local power, P_{satur} is the saturation power. In our case, this dependence can be rewritten as

$$\gamma = \frac{\gamma_0}{1 + \mu_{satur}(s + C/s)},$$

and in the initial relations, formulas (9) and (11) will remain unchanged, while equation (10) should be replaced with

$$\frac{s'}{s} = -\left(\frac{\mu_{satur}(s + C/s)}{1 + \mu_{satur}(s + C/s)} + n\right). \qquad (18)$$

Obviously, in the region with high radiation intensity, the effective medium will become unbalanced, and the layer will absorb the radiation passing through it.

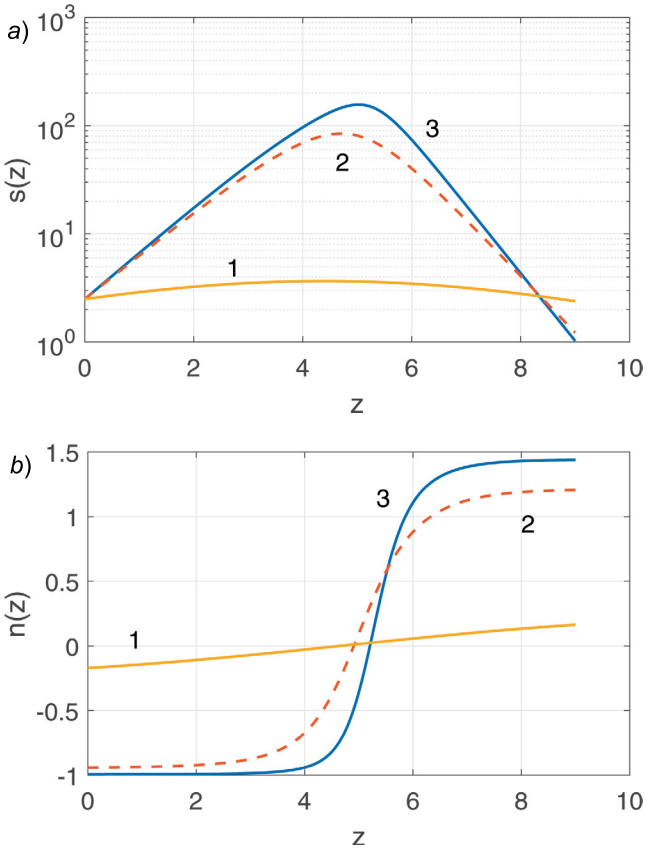

Fig. 4. Structure of bistable solution considering the gain saturation effect: *a* — dependence $s(z)$ (logarithmic scale); *b* — dependence $n(z)$ for three stationary solutions with minimal (curves 1), medium (curves 2, unstable solution) and maximal (curves 3) field gain and particle concentration perturbation within the layer. Comparison with the results in Fig. 3 shows notable smoothing of field and concentration inhomogeneity in the layer and disruption of absorption-gain balance for intense radiation passing through the layer (see curves 2 and 3 in panel a). For numerical modeling, the same parameters were used as in Fig. 3, and saturation parameter $\mu_{satur} = 0.003$

As an example, Fig. 4 shows the solution structure considering the gain saturation effect for the same parameters as in Fig. 3, and the saturation parameter $\mu_{satur} = 0.003$. This nonlinear effect significantly influences solutions with high field intensity, where the balance between absorption and gain is violated. From an experimental perspective in the PT-symmetry domain, this issue can be resolved by increasing pump power so that field intensities at the layer input and output become equal. However, this will lead to an imbalance of gainabsorption for the solution with weak gain and density perturbation, and such input power correction would need to be performed in each individual case.

6. DISCUSSION

Besides one-sided radiation input into the layer, one can also consider the problem setup with radiation launch from both sides of the layer, where it is possible to control not only the amplitudes but also the phase shift $\Delta\phi$ of waves incident from right and left. In this case, almost any amplitude ratio a_+/a_- at the layer boundary can be achieved, as it will be determined not only by the dielectric permittivities of the layer and medium but also by these additional input parameters.

An interesting variant occurs when the parameter $\beta = 1$. In this case, the solution will possess PT-symmetry (dielectric permittivity is odd, and field intensity is an even function z) regardless of the layer thickness and incident radiation amplitude. At high amplitudes, the stationary distribution of particle concentration will approach a step-like profile with zero density in the input half of the layer,

$$N(-L/2 < z < 0) \approx 0,$$

$$n(-L/2 < z < 0) \approx -1,$$

and doubled average particle concentration in the output half,

$$N(0 < z < L/2) \approx 2N_0,$$

$$n\ (0 < z < L/2) \approx 2.$$

The transition region between these values has a finite thickness Δ, while the increase in incident wave power leads to a decrease in Δ. Accordingly, both in relation to the particle concentration distribution and the field intensity profile, the radiation-particle interaction mode reaches saturation, and the distribution $\mathrm{Im}\varepsilon$ tends toward step-like.

In the standard problem with a predetermined step-like profile of the imaginary part of permittivity [20],

$$\mathrm{Im}\varepsilon \sim \theta(z) - 1/2$$

($\theta(z)$ — Heaviside function), increasing layer thickness leads to PT-symmetry breaking and instability emergence, where the boundary between stable and unstable regimes represents an exceptional point in the parameter space (here the parameter is layer thickness). Many important effects for applications are due to the presence of an exceptional point and manifest directly near it. In the problem formulation considered here, the exceptional point effect is difficult to implement since it is associated with energy exchange between two modes a_+ and a_- at the jump $\mathrm{Im}\varepsilon$, and for optical radiation, the jump scale (transition region from absorbing to amplifying medium) Δ must be on the order of wavelength. On the other hand, if a defect is introduced into the layer at some point z_{def} which causes partial reflection and thus mode interaction, then changing the defect magnitude will create an exceptional point in the system. Moreover, in this case, the exceptional point effect is easily controllable but will not be associated with PT-symmetry breaking, rather with the emergence of complex eigenvalues in the spectrum and instability development.

7. CONCLUSIONS

In conclusion, we note that this work studied the interaction of light with a layer of liquid metamaterial, which is a colloidal solution of absorbing nanoparticles in an amplifying liquid (gel) with compensated absorption and amplification. As a result of ponderomotive forces, gradient and drag forces, redistribution of nanoparticle concentration occurs, leading to the appearance of spatially separated regions of light absorption and amplification. It is shown that depending on the intensity of the incident light wave, both smooth PT-symmetric distributions of the effective dielectric permittivity of the colloid and quasi-step distributions, for which PT-symmetry is broken, can occur. The possibility of bistable states emergence is also shown, the realization of which depends on the process prehistory. In all considered cases, the reflection and transmission coefficients of light through the layer do not depend on light intensity and coincide with the "undisturbed" limit of vanishingly small amplitudes of the incident electromagnetic wave due to the absence of interaction between counter-propagating modes inside the layer. The possibility of controlled creation of specified nanoparticle concentration profiles and, consequently, tunable spatial regions of absorption and amplification gives hope that the considered optical system may prove useful for studying non-Hermitian optical effects and diagnosing nanoparticle concentration distribution using probe waves.

FUNDING

This work was supported by the Ministry of Science and Higher Education of the Russian Federation: state tasks FFUF-2023-0002 (sections 4, 5) and FFUF-2024-0019 (other sections).

REFERENCES

1. R. El-Ganainy, K. G. Makris, M. Khajavikhan et al., *Non-Hermitian Physics and Pt Symmetry*, Nature Phys. **14**, 11 (2018).
2. C. M. Bender and S. Boettcher, Real Spectra in *Non-Hermitian Hamiltonians Having PT-Symmetry*, Phys. Rev. Lett. **80**, 5243 (1998).
3. A. A. Zyablovsky, A. P. Vinogradov, A. A. Pukhov, A. V. Dorofeenko, A. A. Lisyansky, *PT-Symmetry in Optics*, Phys. Uspekhi **57**, 1063 (2014).
4. W. D. Heiss, J. Phys. A **37**, 2455 (2004).
5. Y. D. Chong, L. Ge, and A. D. Stone, *PT-Symmetry Breaking and Laser-Absorber Modes in Optical Scattering Systems*, Phys. Rev. Lett. **106**, 093902 (2011).
6. Z. J. Wong, J. Kim, K. O'Brien, Y. Wang, L. Fencs, and X. Zhang, *Lasing and Anti- Lasing in a Single Cavity*, Nature Photon. **10**, 796 (2016).
7. X. Zhu, L. Feng, P. Zhang, X. Yin, and X. Zhang, *One-Way Invisible Cloak Using Parity-Time Symmetric Transformation Optics*, Opt. Lett. **38**, 2821 (2013).
8. W. Chen, S. K. Ozdemir, G. Zhao, J. Wiersig, and L. Yang, *Exceptional Points Enhance Sensing in an Optical Microcavity*, Nature **548**, 192 (2017).
9. M. A. Noginov, G. Zhu, A. M. Belgrave, R. Bakker, V. M. Shalaev, E. E. Narimanov, S. Stout, E. Herz, T. Suteewong, and U. Wiesner, *Demonstration of a Spacer-Based Nanolasers*, Nature Lett. **460**, 1110 (2009).
10. Y. Wu, Zh. Huang, Qi Sun, V. D. Ta, S. Wang, and Y. Wang, *A New Generation of Liquid Lasers from Engineered Semiconductor Nanocrystals with Giant Optical Gain*, Laser Photon. Rev. **17**, 2200703 (2023).
11. A. A. Zharov and N. A. Zharova, *Light-Driven PT-Symmetry in Colloids with Gain and Loss Nanoparticles*, J. Opt. Soc. Am. B **40**, 2618 (2023).
12. D. Gao, R. Shi, Y. Huang, and L. Gao, *Fano-Enhanced Pulling and Pushing Optical Forces on Active Nanoparticles*, Phys. Rev. A **96**, 043826 (2017).
13. H. Chen, L. Gao, C. Zhong, G. Yuan, Y. Huang, Z. Yu, M. Cao, and M. Wang, *Optical Pulling Force on Nonlinear Nanoparticles with Gain*, AIP Advances **10**, 015131 (2020).
14. X. Bian, D. L. Gao, and L. Gao, *Tailoring Optical Pulling Force on Gain Coated Nanoparticles with Nonlocal Effective Medium Theory*, Opt. Express **25**, 24566 (2017).
15. Y. Wu, Z. Huang, Q. Sun, V. D. Ta, S. Wang, and Y. Wang, *A New Generation of Liquid Lasers from Engineered Semiconductor Nanocrystals with Giant Optical Gain*, Laser Photon. Rev. **17**, 2200703 (2023).
16. B. Yang, H. Sun, C.-J. Huang, H.-Y. Wang, Y. Deng, H.-N. Dai, Z.-S. Yuan, and J.-W. Pan, *Cooling and Entangling Ultracold Atoms in Optical Lattices*, Science **369**, 550 (2020).
17. H. Xin, Y. Li, Y.-C. Liu, Y. Zhang, Y.-F. Xiao, and B. Li, *Optical Forces: from Fundamental to Biological Applications*, Adv. Mater. **32**, 2001994 (2020).
18. A. A. Zharov, Jr., A. A. Zharov, I. V. Shadrivov, and N. A. Zharova, *Grading Plasmonic Nanoparticles with Light*, Phys. Rev. A **93**, 013814 (2016).
19. H. Gibbs, *Optical Bistability. Controlling Light with Light*, Mir, Moscow (1988).
20. Y. D. Chong, Li Ge, and A. D. Stone, *PT-Symmetry Breaking and Laser-Absorber Modes in Optical Scattering Systems*, Phys. Rev. Lett. **106**, 093902 (2011).